

# Feedback-voltage driven chaos in three-terminal spin-torque oscillator

Tomohiro Taniguchi<sup>1, a)</sup>

*National Institute of Advanced Industrial Science and Technology (AIST), Research Center for Emerging Computing Technologies, Tsukuba 305-8568, Japan*

(Dated: 18 June 2024)

Recent observations of chaos in nanomagnet suggest a possibility of new spintronics applications such as random-number generator and neuromorphic computing. However, large amount of electric current and/or magnetic field are necessary for the excitation of chaos, which are unsuitable for energy-saving applications. Here, we propose an excitation of chaos in three-terminal spin-torque oscillator (STO). The driving force of the chaos is voltage-controlled magnetic anisotropy (VCMA) effect, which enables us to manipulate magnetization dynamics without spending electric current or magnetic field, and thus, energy efficient. In particular, we focus on the VCMA effect generated by feedback signal from the STO since feedback effect is known to be effective in exciting chaos in dynamical system. Solving the Landau-Lifshitz-Gilbert (LLG) equation numerically and applying temporal and statistical analyses to its solution, the existence of the chaotic and transient-chaotic magnetization dynamics driven by the feedback VCMA effect is identified.

Chaos is a kind of nonlinear dynamics which is sensitive to the initial state and thus, is difficult to predict its time evolution. These characteristics have attracted attention not only from fundamental aspect<sup>1</sup> but also from practical applications such as random-number generator<sup>2</sup>, chaotic communication<sup>3</sup>, and brain-inspired computing<sup>4</sup>. Recent predictions and observations of chaos in nanostructured ferromagnets suggest a possibility to realize these applications by spintronics devices<sup>5–18</sup>. Since chaos can appear only in a high-dimensional phase space<sup>1,19,20</sup>, various methods to increase the number of the dynamical degree of freedom have been used in the previous works, such as injecting periodic signal<sup>6,7,15</sup> and increasing the number of the ferromagnets<sup>5,12</sup>. Among them, adding feedback signal is an efficient approach<sup>21</sup> because feedback effect generally increases the number of the dynamical degree of freedom significantly and thus, makes it easy to excite chaos. A large number of the dynamical degree of freedom is also preferable for practical applications. For example, the number of the linearly independent dynamical degree of freedom bounds the computational capability of physical reservoir computing<sup>22</sup>. Motivated by these reasons, chaos in spin-torque oscillators (STOs) driven by feedback electric current or magnetic field has intensively been investigated both theoretically<sup>13,14,18</sup> and experimentally<sup>16,23</sup>. However, using the feedback electric current causes considerable the Joule heating, and using the feedback magnetic field prevents all-electrical control of devices.

Another candidate as the feedback signal is the voltage-controlled magnetic anisotropy (VCMA) effect<sup>24–26</sup>, where an application of voltage to magnetic tunnel junctions modifies magnetic anisotropy energy by a modulation of electron states<sup>27–29</sup> and/or induction of magnetic moment<sup>30</sup> near ferromagnet metal/insulating barrier interface. The VCMA effect does not, in principle, increase Joule heating and enables the system to

work by all-electrical manipulation. Therefore, it is of great value to examine whether chaos can be excited by the feedback VCMA effect.

In this work, we study an excitation of chaos in a three-terminal STO with feedback VCMA effect by numerical simulations of the Landau-Lifshitz-Gilbert (LLG) equation. An STO is placed on a bottom electrode, which generates spin current through the spin Hall effect<sup>31–34</sup> and drives magnetization oscillation. The electric current flowing in the bottom electrode also generates electric signal reflecting magnetization oscillation through anisotropic magnetoresistance (AMR) effect. The AMR signal is converted to voltage which is then applied to the STO from another terminal. As can be seen, using the three-terminal structure allows us to use the spin-transfer (spin-orbit) torque<sup>35,36</sup> and VCMA effects simultaneously, which enables us to control the magnetization excitation in the STO and the bifurcation from simple to chaotic dynamics independently. This was impossible in two-terminal STOs studied previously. The existence of chaos, as well as transient chaos<sup>37</sup>, caused by the feedback VCMA effect in the three-terminal STO is identified from the temporal solution of the LLG equation and its statistical analyses.

Figure 1 is a schematic illustration of a three-terminal STO, where electric current density  $J$  flowing in a bottom electrode (along the  $x$  direction) generates spin current polarized in the  $y$  direction and injected into the STO. The spin current excites spin-transfer (spin-orbit) torque on magnetization in a free layer. The magnetization oscillation can be detected by AMR effect, as in the case of spin-torque ferromagnetic resonance experiments in three-terminal structures<sup>38</sup>. Then, this AMR signal is sent to the other terminal through a feedback circuit and is used to determine the feedback voltage, as shown in Fig. 1. Therefore, both the spin Hall and VCMA effects coexist in this structure. We should mention here that the possibility of utilizing both of them simultaneously was experimentally confirmed in three-terminal magnetoresistive memory<sup>39</sup>. In the present work, the magni-

<sup>a)</sup>Electronic mail: tomohiro-taniguchi@aist.go.jp

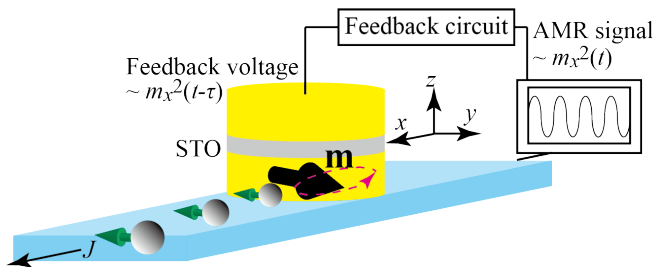


FIG. 1. Schematic illustration of three-terminal STO with feedback voltage. Electric current density  $J$  flowing in the  $x$  direction generates spin current polarized in the  $y$  direction and is injected in the STO. The spin current excites spin-transfer (spin-orbit) torque on the magnetization  $\mathbf{m}$  of a (bottom) free layer in the STO and induces magnetization oscillation around the  $y$  axis. The electric current density in the bottom electrode also generates AMR signal ( $\propto m_x^2$ ), which passes through feedback circuit with delay time  $\tau$  and is converted to feedback voltage applied to the STO from another terminal.

TABLE I. Parameters used in the numerical calculations:  $M$ , saturation magnetization;  $H_K$ , in-plane magnetic anisotropy field;  $\gamma$ , gyromagnetic ratio;  $\alpha$ , Gilbert damping constant;  $d$ , thickness of the free layer;  $\vartheta$ , spin Hall angle;  $J$ , current density;  $\tau$ , delay time.

Quantity	Value
$M$	1000 emu/cm <sup>3</sup>
$H_K$	200 Oe
$\gamma$	$1.764 \times 10^7$ rad/(Oe s)
$\alpha$	0.010
$d$	2 nm
$\vartheta$	0.34
$J$	15 MA/cm <sup>2</sup>
$\tau$	20 ns

tude of the voltage for this VCMA effect is determined by the feedback signal. The advantage and/or necessity to use three-terminal structures, rather than two-terminal STOs, in the present study will also be discussed at the end of this paper. Note also that the feedback circuit can amplify or attenuate the input signal and yield a delay time  $\tau$ <sup>16,23</sup>, where a typical value of  $\tau$  available in experiments is on the order of 1-10 ns.

The magnetization dynamics in the proposed STO is described by the LLG equation given by

$$\frac{d\mathbf{m}}{dt} = -\gamma \mathbf{m} \times \mathbf{H} - \frac{\gamma \hbar \vartheta J}{2eMd} \mathbf{m} \times (\mathbf{e}_y \times \mathbf{m}) + \alpha \mathbf{m} \times \frac{d\mathbf{m}}{dt}, \quad (1)$$

where  $\mathbf{m} = (m_x, m_y, m_z)$  is the unit vector pointing in the direction of the magnetization in the free layer, while  $\mathbf{e}_k$  ( $k = x, y, z$ ) is the unit vector in the  $k$  direction. The gyromagnetic ratio, saturation magnetization, thickness along the  $z$  direction, and the Gilbert damping constant of the free layer are denoted as  $\gamma$ ,  $M$ ,  $d$ , and  $\alpha$ , respectively. The spin Hall angle is  $\vartheta$ . We assume that the free layer in the STO is in-plane magnetized and its magnetic field  $\mathbf{H}$  is given by

$$\mathbf{H} = H_K m_y \mathbf{e}_y - 4\pi M \{1 + \nu [m_x(t - \tau)]^2\} m_z \mathbf{e}_z, \quad (2)$$

where  $H_K$  is the in-plane magnetic anisotropy field along the  $y$  direction while  $4\pi M$  is the demagnetization field along the  $z$  direction. The term  $\nu [m_x(t - \tau)]^2$  represents the modulation of the perpendicular magnetic anisotropy field by the VCMA effect, where the magnitude of the modulation is determined by the AMR feedback signal proportional to  $m_x^2$ . The dimensionless coefficient  $\nu$  is defined as  $H_{K,V}/(4\pi M)$ , where  $H_{K,V} = 2\eta V/(Mdd_1)$  represents the magnitude of the VCMA effect in terms of magnetic field with the VCMA efficiency  $\eta$ , voltage  $V$ , and the thickness  $d_1$  of the insulating layer in the STO. The VCMA efficiency recently obtained in the experiment reaches about 300 fJ/(V m)<sup>40</sup>, which makes  $H_{K,V}$  be on the order of kilo Oersted for typical device structures. The magnitude of the voltage,  $|V|$ , which might include an amplification or attenuation by the feedback circuit, is limited to be about 0.5 V at maximum to avoid electrostatic breakdown of the STO. The saturation magnetization  $M$  in typical STOs and/or VCMA devices are about 1000 emu/cm<sup>3</sup>. Regarding these values, the magnitude of  $\nu$  can be on the order of 0.1. The values of the parameters used in the following calculations, except  $\nu$ , are summarized in Table I. We solved Eq. (1) with an initial condition  $\mathbf{m}(0) = (\sin 90^\circ \cos 89^\circ, \sin 90^\circ \sin 89^\circ, \cos 90^\circ)$  from  $t = 0$  to  $t = t_{\max}$ , where  $t_{\max} = 1.0 \mu\text{s}$  throughout this work. As a general consequence for chaos and transient chaos<sup>37</sup>, the results shown below, such as their boundary, depend on the choice of  $t_{\max}$ , which will be discussed later. The fourth-order Runge-Kutta method extended to feedback system<sup>14,41</sup> was applied for solving Eq. (1), where the time increment of the LLG equation is defined from the delay time  $\tau$  and an integer  $N$  as  $\Delta t = \tau/N$  ( $N = 2 \times 10^4$ , or equivalently,  $\Delta t = 1$  ps, in this work). For the latter discussion, we note that the number of the dynamical degree of the freedom in this numerical scheme is  $2(N + 1)$ <sup>14,41</sup>.

Figures 2(a)-2(c) summarize typical dynamics of  $m_x$  (red) and  $m_y$  (blue) near  $t = 0$ , where  $\nu$  is (a) 0, (b) 0.1, and (c) 0.5, while the Fourier spectra,  $|m_x(f)|$ , of  $m_x(t)$  for these  $\nu$  are shown in Figs. 2(d)-2(f). The Fourier spectra for various  $\nu$  are summarized in Fig. 3. In the absence of the feedback effect ( $\nu = 0$ ), an auto-oscillation with a single main frequency is excited, as in the case of the conventional three-terminal STOs<sup>42</sup>; see Figs. 2(a) and 2(d), as well as the inset in Fig. 2(a). In the presence of the feedback effect, however, the dynamics is largely modulated, although the dynamics during a short time scale looks similar to a simple auto-oscillation; see Fig. 2(b) and compare the insets in Fig. 2(a) and 2(b). The complexity of the dynamics is also found from the Fourier spectrum in Fig. 2(e), where the spectra shows broadened structure. The magnetization switching is also observed for some values of  $\nu$ , as shown in Fig. 2(c). Note that the oscillation amplitude repeats amplification and reduction before the switching, which is also reflected in the broadened structure of the Fourier spectrum in Fig. 2(f). This switching behavior is quite different from the conventional spin-transfer

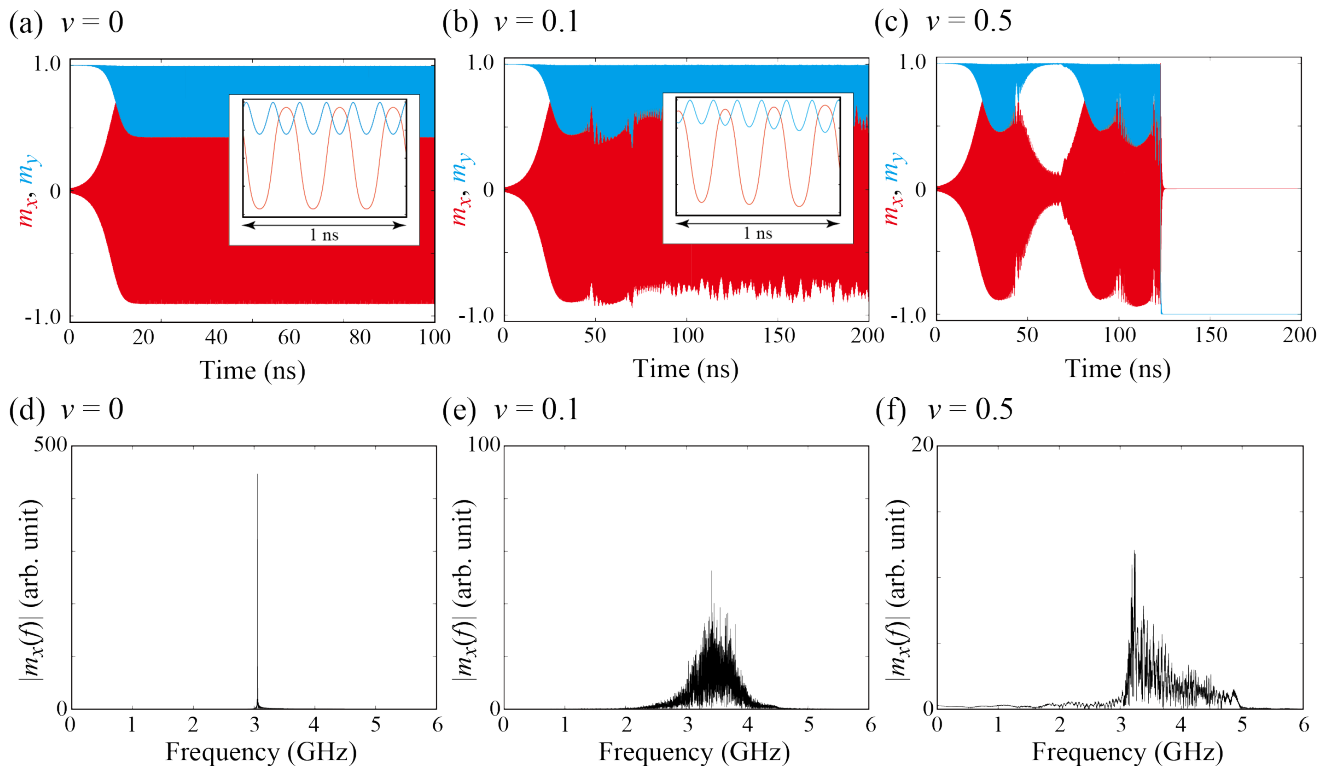


FIG. 2. Temporal dynamics of  $m_x$  and  $m_y$  for  $\nu$  of (a) 0, (b) 0.1, and (c) 0.5. The insets in (a) and (b) show their dynamics in a time range of 1 ns. Fourier spectra,  $|m_x(f)|$ , of  $m_x(t)$  for those  $\nu$  are shown in (d)-(f).

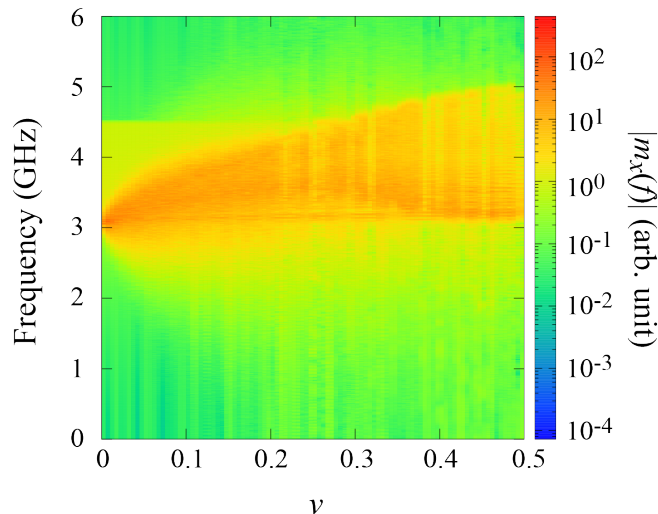


FIG. 3. Power spectrum density,  $|m_x(f)|$ , for various  $\nu$ , where  $m_x(f)$  is the Fourier transformation of  $m_x(t)$ .

(spin-orbit) torque switching<sup>43</sup>, where the work done by the spin-transfer torque monotonically supply energy into the ferromagnet and thus, the oscillation amplitude also increases monotonically. The complex behavior before the magnetization switching found in Fig. 2(c) suggest that the dynamics is classified as transient chaos<sup>37</sup>, where nonlinear dynamical system shows chaotic behavior before saturating to a fixed point.

Summarizing the results, it is shown that the feedback VCMA effect causes the modulation of the oscillation amplitude in the STO, and the dynamics becomes complex. The complexity of the dynamics results in the broadened structure of the Fourier spectra, as summarized in Fig. 3. These results are similar to the characteristics found in chaotic spintronics devices with feedback current or magnetic field<sup>14,16,18</sup>. We should, however, recall that an appearance of complex dynamics is not a direct evidence of the existence of chaos. Although the complexity of dynamics is a typical characteristic of chaos, not all complex dynamics is classified as chaos. Therefore, to identify chaos, we evaluate the Lyapunov exponent<sup>1</sup>.

The Lyapunov exponent is an expansion rate of a distance between two solutions of the LLG equation having an infinitesimally different initial conditions. Let us denote the solution of the LLG equation with an initial condition  $\mathbf{m}$  [ $\mathbf{m}(t)$ ,  $\mathbf{m}(t - \Delta t)$ ,  $\dots$ ,  $\mathbf{m}(t - \tau)$ ] for performing the numerical simulation, where  $\mathbf{m}(t - \Delta t)$ ,  $\dots$ ,  $\mathbf{m}(t - \tau)$  are the past values of  $\mathbf{m}(t)$  and are used as feedback signal. To evaluate the Lyapunov exponent, for each  $\mathbf{m}(t - k\Delta t)$  ( $k = 0, 1, \dots, N$ ), we introduce the zenith and azimuth angles,  $\theta_k = \cos^{-1} m_z(t - k\Delta t)$  and  $\varphi_k = \tan^{-1}[m_y(t - k\Delta t)/m_x(t - k\Delta t)]$ . Then, we introduce  $\tilde{\mathbf{m}}(t - k\Delta t)$ , whose zenith and azimuth angles,  $\tilde{\theta}_k = \cos^{-1} \tilde{m}_z(t - k\Delta t)$  and  $\tilde{\varphi}_k = \tan^{-1}[\tilde{m}_y(t - k\Delta t)/\tilde{m}_x(t - k\Delta t)]$ , are defined by shifting  $\theta_k$  and  $\varphi_k$  with infinitesimal differences ( $|\epsilon_{k,\theta}|, |\epsilon_{k,\varphi}| \ll 1$ ) as  $\tilde{\theta}_k = \theta_k + \epsilon_{k,\theta}$  and  $\tilde{\varphi}_k = \varphi_k + \epsilon_{k,\varphi}$ .

Therefore, the distance between  $\mathbf{m}(t - k\Delta t)$  and  $\tilde{\mathbf{m}}(t - k\Delta t)$  at time  $t$  is given by  $\epsilon_k = \sqrt{\epsilon_{k,\theta}^2 + \epsilon_{k,\varphi}^2}$ , and their sum is  $\epsilon = \sum_{k=0}^N \epsilon_k$ . Then, we evaluate the time evolution of  $\mathbf{m}(t)$  and  $\tilde{\mathbf{m}}(t)$  from time  $t$  to  $t + \Delta t$  by solving the LLG equation and obtain  $\mathbf{m}(t + \Delta t)$  and  $\tilde{\mathbf{m}}(t + \Delta t)$ . Note that the distance  $\epsilon'_0$  between these  $\mathbf{m}(t + \Delta t)$  and  $\tilde{\mathbf{m}}(t + \Delta t)$ , in terms of  $\theta'_0 = \cos^{-1} m_z(t + \Delta t)$ ,  $\varphi'_0 = \tan^{-1}[m_y(t + \Delta t)/m_x(t + \Delta t)]$ ,  $\tilde{\theta}'_0 = \cos^{-1} \tilde{m}_z(t + \Delta t)$ , and  $\tilde{\varphi}'_0 = \tan^{-1}[\tilde{m}_y(t + \Delta t)/\tilde{m}_x(t + \Delta t)]$ , is generally different from that,  $\epsilon_0$ , between  $\mathbf{m}(t)$  and  $\tilde{\mathbf{m}}(t)$ . Then, defining  $\epsilon' = \epsilon - \epsilon_0 + \epsilon'_0$ , the expansion rate of the solution of the LLG equation during  $[t, t + \Delta t]$  is given by  $\epsilon'/\epsilon$ . Therefore, a temporal Lyapunov exponent at time  $t + \Delta t$  is defined as

$$\lambda = \frac{1}{\Delta t} \ln \frac{\epsilon'}{\epsilon}. \quad (3)$$

We repeat this procedure and evaluate the temporal Lyapunov exponent at every time from  $t = \tau$ . Finally, the Lyapunov exponent  $\Lambda$  is defined as a statistical average of the temporal Lyapunov exponents as  $\Lambda = (1/\mathcal{N}) \sum_{i=1}^{\mathcal{N}} \lambda_i$ , where  $\mathcal{N}$  is the number of the averaging and  $\lambda_i$  is the  $i$ th temporal Lyapunov exponent; see also Ref.<sup>14</sup>, which refers to how to define the Lyapunov exponent in feedback system. The sign of the Lyapunov exponent indicates the dynamical state of the system, i.e., negative exponent corresponds to dynamics saturating to a fixed point, zero exponent corresponds to a periodic dynamics, and positive exponent corresponds to chaos. Figure 4 summarizes the Lyapunov exponent for various  $\nu$ . The value is zero at  $\nu = 0$ , i.e., in the absence of the feedback effect, because the magnetization dynamics in this case is a periodic oscillation (auto-oscillation), as shown in Fig. 2(a). For finite feedback effect ( $\nu \neq 0$ ), such as the dynamics in Fig. 2(b), the Lyapunov exponent becomes positive, which can be an evidence of the existence of chaos in the present system. The Lyapunov exponent can also be negative for some  $\nu$  when the magnetization switches its direction, as shown in Fig. 2(c). Summarizing them, the sign of the Lyapunov exponent reasonably reflects the dynamical behavior of the magnetization.

Note that analyses on both temporal dynamics in Fig. 2 and statistical property (Lyapunov exponent) in Fig. 4 are necessary to identify dynamical state of the magnetization. The temporal analysis clarifies the existence of complex dynamics, at least as temporary, which might be missed from the Lyapunov exponent. For example, for the dynamics shown in Fig. 2(c), chaotic behavior appeared initially might be missed when only the Lyapunov exponent is evaluated. On the other hand, the evaluation of the Lyapunov exponent can be used as a figure of merit to distinguish between chaos and complex but non-chaotic dynamics, which is hard to determine from just observing temporal dynamics. While the temporal dynamics in STOs has been frequently measured and used in practical applications<sup>44</sup>, one may be interested in how

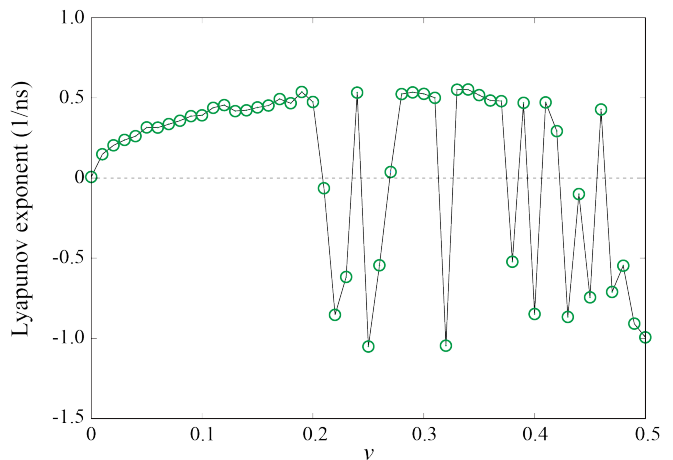


FIG. 4. Lyapunov exponent for various  $\nu$ . A horizontal dotted line is added as a guide for eyes to clarify a boundary of zero exponent.

to estimate the Lyapunov exponent experimentally. In experiments, it is difficult to control the initial state of the magnetization, and thus, the evaluation method of the Lyapunov exponent used in the numerical simulation is hardly applicable. There are, however, various methods to estimate the Lyapunov exponent from experimental data by reproducing the dynamical trajectory in an embedded space<sup>19</sup> or identify chaos from different quantities, such as noise limit<sup>9,16,45,46</sup>. Therefore, it will be possible to examine the validity of the present results by experiments in future.

Recall that the identification of chaos sometimes depends on the measurement time  $t_{\max}$ , especially when transient chaos possibly occurs<sup>37</sup>. For example, we did not observe magnetization switching until  $t_{\max} = 1 \mu\text{s}$  for  $\nu = 0.1$  shown in Fig. 2(b); therefore, the corresponding Lyapunov exponent for this  $\nu$  is positive, as shown in Fig. 4. If we use, however,  $t_{\max}$  longer than  $1 \mu\text{s}$ , a switching might occur; in this case, the Lyapunov exponent will be negative and the dynamics will be classified as transient chaos. On the other hand, if we, for example, use  $t_{\max} = 100 \text{ ns}$ , the dynamics for  $\nu = 0.5$  shown in Fig. 2(c) might be classified as chaos and the Lyapunov exponent becomes positive because at  $t = 100 \text{ ns}$ , the switching does not occur. As shown in these examples, the identification of chaos depends on the measurement time. This is not a particular property for spintronics devices; rather, this is a general consequence in chaotic system<sup>37</sup>. It is generally difficult to estimate the transient time, if transient chaos exists, because it depends not only on the values of parameters but also on the initial conditions and so on<sup>37</sup>. The time scale during which chaos can be kept determines the manipulation time of chaos applications, and thus, is of great interest. We keep this issue as a future work.

At the end of this work, let us mention advantage and/or necessity using the three-terminal structure, instead of the two-terminal one studied

previously<sup>13,14,16,18,23</sup>. The three-terminal structure allows us to utilize both the spin-transfer torque and VCMA effects simultaneously<sup>39</sup>, as mentioned earlier. In the two-terminal device, these effects hardly coexist because their source current and voltage are not independent from each other, and they require contradicting conditions for resistance of the device. The spin-transfer torque effect arises from a flow of electrons<sup>35,36</sup>, while the VCMA effect arises from an accumulation of electrons<sup>28,29</sup>. Thus, the resistances of the spin-transfer torque and VCMA devices are greatly different. For example, the resistance of an STO in Ref.<sup>47</sup> is at least one or two orders of magnitude smaller than that of the VCMA devices<sup>48</sup>. Accordingly, it is difficult to fabricate devices in which two effects coexist. Although small current can flow even in VCMA devices for reading the magnetization direction, it is not sufficient for the current required in STOs applications<sup>49</sup>. The three-terminal structure solves this contradiction by separating the paths of the electric current generating the spin-transfer torque and the voltage for the VCMA effect.

In summary, we proposed a three-terminal STO with feedback VCMA effect. The spin Hall effect in the bottom electrode results in an auto-oscillation of the magnetization in the STO. The magnetization oscillation can be detected by the AMR effect, whose signal is sent to another terminal and is converted to the feedback voltage. The feedback VCMA effect induces chaos in the STO without generating Joule heating or without applying magnetic field. Therefore, the proposed structure will be an attractive candidate for applying spintronics technology to practical applications utilizing chaos. The three terminal structure is necessary for allowing the coexistence of the spin-transfer (spin-orbit) torque and VCMA effects, where the former drives the magnetization oscillation while the latter makes it chaotic. The existence of chaos, as well as transient chaos, in this STO was confirmed by solving the LLG equation numerically and applying temporal and statistical analyses to its solution.

The work is supported by JSPS KAKENHI Grant Number 20H05655 and 24K01336.

## AUTHOR DECLARATIONS

### Conflict of Interest

The authors have no conflicts to disclose.

## AUTHOR CONTRIBUTIONS

Tomohiro Taniguchi: Conceptualization, Investigation, Visualization, Writing

## DATA AVAILABILITY

The data that support the findings of this study are available from the corresponding author upon reasonable request.

- <sup>1</sup>S. H. Strogatz, *Nonlinear Dynamics and Chaos: With Applications to Physics, Biology, Chemistry, and Engineering*, 1st ed. (Westview Press, Boulder, 2001).
- <sup>2</sup>T. Stojanovski and L. Kocarev, "Chaos-based random number generators-part I: analysis," *IEEE Trans. Circuits Syst. I: Fundamental and Theory* **48**, 281 (2001).
- <sup>3</sup>K. M. Cuomo and A. V. Oppenheim, "Circuit Implementation of Synchronized Chaos, with Applications to Communications," *Phys. Rev. Lett.* **71**, 65 (1993).
- <sup>4</sup>D. Verstraeten, B. Schrauwen, M. D'Haene, and D. Stroobandt, "An experimental unification of reservoir computing methods," *Neural Netw.* **20**, 391 (2007).
- <sup>5</sup>K. Kudo, R. Sato, and K. Mizushima, "Synchronized Magnetization Oscillations in F/N/F Nanopillars," *Jpn. J. Appl. Phys.* **45**, 3869 (2006).
- <sup>6</sup>Z. Li, Y. C. Li, and S. Zhang, "Dynamic magnetization states of a spin valve in the presence of dc and ac currents: Synchronization, modification, and chaos," *Phys. Rev. B* **74**, 054417 (2006).
- <sup>7</sup>Z. Yang, S. Zhang, and Y. C. Li, "Chaotic Dynamics of Spin-Valve Oscillators," *Phys. Rev. Lett.* **99**, 134101 (2007).
- <sup>8</sup>S. Petit-Watelot, J.-V. Kim, A. Ruotolo, R. M. Otxoa, K. Bouzehouane, J. Grollier, A. Vansteenkiste, B. V. de Wiele, V. Cros, and T. Devolder, "Commensurability and chaos in magnetic vortex oscillations," *Nat. Phys.* **8**, 682–687 (2012).
- <sup>9</sup>T. Devolder, D. Rontani, S. Petit-Watelot, K. Bouzehouane, S. Andrieu, J. Letang, M.-W. Yoo, J.-P. Adam, C. Chappert, S. Girod, V. Cros, M. Sciamanna, and J.-V. Kim, "Chaos in magnetic nanocontact vortex oscillators," *Phys. Rev. Lett.* **123**, 147701 (2019).
- <sup>10</sup>A. V. Bondarenko, E. Holmgren, Z. W. Li, B. A. Ivanov, and V. Korenivski, "Chaotic dynamics in spin-vortex pairs," *Phys. Rev. B* **99**, 054402 (2019).
- <sup>11</sup>E. A. Montoya, S. Perna, Y.-J. Chen, J. A. Katine, M. d'Aquino, C. Serpico, and I. N. Krivorotov, "Magnetization reversal driven by low dimensional chaos in a nanoscale ferromagnet," *Nat. Commun.* **10**, 543 (2019).
- <sup>12</sup>T. Taniguchi, "Synchronized, periodic, and chaotic dynamics in spin torque oscillator with two free layers," *J. Magn. Magn. Mater.* **483**, 281–292 (2019).
- <sup>13</sup>J. Williams, A. D. Accoily, D. Rontani, M. Sciamanna, and J.-V. Kim, "Chaotic dynamics in a macrospin spin-torque nano-oscillator with delayed feedback," *Appl. Phys. Lett.* **114**, 232405 (2019).
- <sup>14</sup>T. Taniguchi, N. Akashi, H. Notsu, M. Kimura, H. Tsukahara, and K. Nakajima, "Chaos in nanomagnet via feedback current," *Phys. Rev. B* **100**, 174425 (2019).
- <sup>15</sup>T. Yamaguchi, N. Akashi, K. Nakajima, S. Tsunegi, H. Kubota, and T. Taniguchi, "Synchronization and chaos in a spin-torque oscillator with a perpendicularly magnetized free layer," *Phys. Rev. B* **100**, 224422 (2019).
- <sup>16</sup>A. Kamimaki, T. Kubota, S. Tsunegi, K. Nakajima, T. Taniguchi, J. Grollier, V. Cros, K. Yakushiji, A. Fukushima, S. Yuasa, and H. Kubota, "Chaos in spin-torque oscillator with feedback circuit," *Phys. Rev. Research* **3**, 043216 (2021).
- <sup>17</sup>T. Taniguchi, "Bifurcation to complex dynamics in largely modulated voltage-controlled parametric oscillator," *Sci. Rep.* **14**, 2891 (2024).
- <sup>18</sup>T. Taniguchi, "Chaotic magnetization dynamics driven by feedback magnetic field," *Phys. Rev. B* **109**, 214412 (2024).
- <sup>19</sup>K. T. Alligood, T. D. Sauer, and J. A. Yorke, *Chaos. An Introduction to Dynamical Systems* (Springer (New York), 1997).
- <sup>20</sup>E. Ott, *Chaos in Dynamical Systems*, 2nd ed. (Cambridge University Press (Cambridge), 2002).

- <sup>21</sup>D. Biswas and T. Banerjee, *Time-Delayed Chaotic Dynamical Systems: From Theory to Electronic Experiment*, 2nd ed. (Springer Cham, 2018).
- <sup>22</sup>T. Kubota, H. Takahashi, and K. Nakajima, “Unifying framework for information processing in stochastically driven dynamical systems,” *Phys. Rev. Research* **3**, 043135 (2021).
- <sup>23</sup>S. Tsunegi, T. Kubota, A. Kamimaki, J. Grollier, V. Cros, K. Yakushiji, A. Fukushima, S. Yuasa, H. Kubota, K. Nakajima, and T. Taniguchi, “Information Processing Capacity of Spintronic Oscillator,” *Adv. Intell. Syst.* **5**, 2300175 (2023).
- <sup>24</sup>M. Weisheit, S. Fähler, A. Marty, Y. Souche, C. Poinsignon, and D. Givord, “Electric Field-Induced Modification of Magnetism in Thin-Film Ferromagnets,” *Science* **315**, 349 (2007).
- <sup>25</sup>T. Maruyama, Y. Shiota, T. Nozaki, K. Ohta, N. Toda, M. Mizuguchi, A. A. Tulapurkar, T. Shinjo, M. Shiraishi, S. Mizukami, Y. Ando, and Y. Suzuki, “Large voltage-induced magnetic anisotropy change in a few atomic layers of iron,” *Nat. Nanotechnol.* **4**, 158 (2009).
- <sup>26</sup>Y. Shiota, T. Maruyama, T. Nozaki, T. Shinjo, M. Shiraishi, and Y. Suzuki, “Voltage-Assisted Magnetization Switching in Ultrathin Fe<sub>80</sub>Co<sub>20</sub> Alloy Layers,” *Appl. Phys. Express* **2**, 063001 (2009).
- <sup>27</sup>C.-G. Duan, J. P. Velez, R. F. Sabirianov, Z. Zhu, J. Chu, S. S. Jaswal, and E. Y. Tsymlal, “Surface Magnetoelectric Effect in Ferromagnetic Metal Films,” *Phys. Rev. Lett.* **101**, 137201 (2008).
- <sup>28</sup>K. Nakamura, R. Shimabukuro, Y. Fujiwara, T. Akiyama, T. Ito, and A. J. Freeman, “Giant Modification of the Magnetocrystalline Anisotropy in Transition-Metal Monolayers by an External Electric Field,” *Phys. Rev. Lett.* **102**, 187201 (2009).
- <sup>29</sup>M. Tsujikawa and T. Oda, “Finite Electric Field Effects in the Large Perpendicular Magnetic Anisotropy Surface Pt/Fe/Pt(001): A First-Principles Study,” *Phys. Rev. Lett.* **102**, 247203 (2009).
- <sup>30</sup>S. Miwa, M. Suzuki, M. Tsujikawa, K. Matsuda, T. Nozaki, K. Tanaka, T. Tsukahara, K. Nawaoka, M. Goto, Y. Kotani, T. Ohkubo, F. Bonell, F. Tamura, K. Hono, T. Nakamura, M. Shirai, S. Yuasa, and Y. Suzuki, “Voltage controlled interfacial magnetism through platinum orbits,” *Nat. Commun.* **8**, 15848 (2017).
- <sup>31</sup>M. I. Dyakonov and V. I. Perel, “Current-induced spin orientation of electrons in semiconductors,” *Phys. Lett. A* **35**, 459 (1971).
- <sup>32</sup>J. E. Hirsch, “Spin Hall Effect,” *Phys. Rev. Lett.* **83**, 1834 (1999).
- <sup>33</sup>S. Zhang, “Spin Hall Effect in the Presence of Spin Diffusion,” *Phys. Rev. Lett.* **85**, 393 (2000).
- <sup>34</sup>Y. K. Kato, R. C. Myers, A. C. Gossard, and D. D. Awschalom, “Observation of the Spin Hall Effect in Semiconductors,” *Science* **306**, 1910 (2004).
- <sup>35</sup>J. C. Slonczewski, “Current-driven excitation of magnetic multilayers,” *J. Magn. Magn. Mater.* **159**, L1 (1996).
- <sup>36</sup>L. Berger, “Emission of spin waves by a magnetic multilayer traversed by a current,” *Phys. Rev. B* **54**, 9353 (1996).
- <sup>37</sup>Y.-C. Lai and T. Tél, *Transient Chaos* (Springer (New York), 2011).
- <sup>38</sup>L. Liu, T. Moriyama, D. C. Ralph, and R. A. Buhrman, “Spin-Torque Ferromagnetic Resonance Induced by the Spin Hall Effect,” *Phys. Rev. Lett.* **106**, 036601 (2011).
- <sup>39</sup>S. Shirotori, H. Yoda, Y. Ohsawa, N. Shimomura, T. Inokuchi, Y. Kato, Y. Kamiguchi, K. Koi, K. Ikegami, H. Sugiyama, M. Shimizu, B. Altansargai, S. Oikawa, M. Ishikawa, A. Tiwari, Y. Saito, and A. Kurobe, “Voltage-Control Spintronics Memory With a Self-Aligned Heavy-Metal Electrode,” *IEEE Trans. Magn.* **53**, 3401104 (2017).
- <sup>40</sup>T. Nozaki, M. Endo, M. Tsujikawa, T. Yamamoto, T. Nozaki, M. Konoto, H. Ohmori, Y. Higo, H. Kubota, A. Fukushima, M. Hosomi, M. Shirai, Y. Suzuki, and S. Yuasa, “Voltage-controlled magnetic anisotropy in an ultrathin Ir-doped Fe layer with a CoFe termination layer,” *APL Mater.* **8**, 011108 (2020).
- <sup>41</sup>E. Hairer and S. P. N. G. Wanner, *Solving Ordinary Differential Equations I: Nonstiff Problems*, 2nd ed. (Springer-Verlag, 1993).
- <sup>42</sup>L. Liu, C.-F. Pai, D. C. Ralph, and R. A. Buhrman, “Magnetic Oscillation Driven by the Spin Hall Effect in 3-Terminal Magnetic Tunnel Junction Devices,” *Phys. Rev. Lett.* **109**, 186602 (2012).
- <sup>43</sup>T. Taniguchi, S. Isogami, Y. Shiokawa, Y. Ishitani, E. Komura, T. Sasaki, S. Mitani, and M. Hayashi, “Magnetization switching probability in the dynamical switching regime driven by spin-transfer torque,” *Phys. Rev. B* **106**, 104431 (2022).
- <sup>44</sup>S. Tsunegi, T. Taniguchi, S. Miwa, K. Nakajima, K. Yakushiji, A. Fukushima, S. Yuasa, and H. Kubota, “Evaluation of memory capacity of spin torque oscillator for recurrent neural networks,” *Jpn. J. Appl. Phys.* **57**, 120307 (2018).
- <sup>45</sup>M. Barahona and C.-S. Poon, “Detection of nonlinear dynamics in short, noisy time series,” *Nature* **381**, 215–217 (1996).
- <sup>46</sup>C.-S. Poon and M. Barahona, “Titration of chaos with added noise,” *Proc. Natl. Acad. Sci. U.S.A.* **98**, 7107 (2001).
- <sup>47</sup>H. Kubota, K. Yakushiji, A. Fukushima, S. Tamaru, M. Konoto, T. Nozaki, S. Ishibashi, T. Saruya, S. Yuasa, T. Taniguchi, H. Arai, and H. Imamura, “Spin-Torque Oscillator Based on Magnetic Tunnel Junction with a Perpendicularly Magnetized Free Layer and In-plane Magnetized Polarizer,” *Appl. Phys. Express* **6**, 103003 (2013).
- <sup>48</sup>Y. Shiota, T. Nozaki, S. Tamaru, K. Yakushiji, H. Kubota, A. Fukushima, S. Yuasa, and Y. Suzuki, “Reduction in write error rate of voltage-driven dynamic magnetization switching by improving thermal stability factor,” *Appl. Phys. Lett.* **111**, 022408 (2017).
- <sup>49</sup>T. Taniguchi, A. Ogihara, Y. Utsumi, and S. Tsunegi, “Spintronic reservoir computing without driving current or magnetic field,” *Sci. Rep.* **12**, 10627 (2022).